Available online at www.sciencedirect.com
SCIENCE DIRECT®
Surface Science 566–568 (2004) 272–277
SURFACE SCIENCE
www.elsevier.com/locate/susc

Ultrathin epitaxial bcc-Co films stabilized on Au(0 0 1)-*hex*

N. Spiridis [a], T. Ślęzak [b], M. Zajac [b], J. Korecki [a,b,*]

[a] *Institute of Catalysis and Surface Chemistry, Polish Academy of Sciences, Niezapominajek 8, 30-239 Kraków, Poland*
[b] *Faculty of Physics and Nuclear Techniques, AGH University of Science and Technology, Al. Mickiewicza 30, 30-059 Kraków, Poland*

Available online 7 June 2004

Abstract

Ultrathin (8 and 16 Å) epitaxial Co films were grown on Au(0 0 1)-*hex* substrates. The films were characterized in situ by LEED, STM and the directional Auger electron spectroscopy (DAES) and ex situ by magnetooptic Kerr effect. From LEED and DAES data it was found that a distorted bcc-Co phase can be stabilized on Au(0 0 1)-*hex* at least up to 10 ML. The easy axis of magnetization for the bcc-Co films coated with Au lies in-plane along a ⟨1 0 0⟩ direction.

Keywords: Low energy electron diffraction (LEED); Auger electron spectroscopy; Scanning tunneling microscopy; Epitaxy; Growth; Cobalt; Gold

1. Introduction

One of the crystallographic phases that do not exist naturally but can be stabilized by epitaxy is metastable bcc-Co. It was obtained for the first time by Prinz [1] on GaAs(1 1 0). Exceptionally thick (357 Å) bcc Co film could be stabilized probably thanks to its nanocrystalline character [2]. It means that the magnetic and hyperfine properties found by Riedi et al. [3] for this sample were not representative for a tru bcc Co-phase. There is still a lot of controversy around the structural and magnetic properties of Co films on GaAs(1 1 0) [4] and GaAs(0 0 1) [5] due to their complicated microstructure [6], inhomogeneities [7] and chemical interdiffusion [8], which is certainly important for ultrathin films [9]. The second commonly exploited substrate for the growth of bcc-Co is Fe(0 0 1), which was used for the ultrathin films [10–12] as well as for multilayer [13,14] growth. On Fe(0 0 1) Co grows as strained bcc-phase [11,12], which is actually body-centered tetragonal up to a critical thickness between 10 and 25 monolayers. In multilayers the metastable phase is stabilized additionally by a Fe overlayer [13]. The structure determination of ultrathin films were done usually by electron diffraction methods, whereas for multilayers NMR showed up to be very helpful clearly identifying and resolving fcc, hcp and bcc cobalt phases [13]. However, NMR, by involving the hyperfine interactions, is sensitive to the proximity of magnetic moments of the substrate when Co is grown on Fe(0 0 1), which may shift the hyperfine magnetic field values. Similarly, the magnetization background coming from iron in Co/Fe systems makes determination of the magnetic properties for bcc-Co difficult.

* Corresponding author. Address: Faculty of Physics and Nuclear Techniques, AGH University of Science and Technology, Al. Mickiewicza 30, 30-059 Kraków, Poland. Tel.: +48-12-617-2911; fax: +48-12-634-1247.
E-mail address: korecki@uci.agh.edu.pl (J. Korecki).

0039-6028/$ - see front matter
doi:10.1016/j.susc.2004.05.056

It becomes then essential to grow bcc-Co on a non-magnetic metallic substrate. Till now bcc-Co films were grown on the (0 1 0) surface of tetragonal TiAl [15] and cubic FeAl [16]. From our point of view promising perspectives of growing and studying Co films was offered by a Au(0 0 1)-*hex* substrate, which we recently have used to grow Fe films [17]. The close analogy between bcc-Co and bcc-Fe structural properties [18] allowed us to expect similar growth modes, mediated by the surfactant Au action [17,19]. Moreover, Wu et al. [20] reported that they were able to stabilize bcc-Co in Co/Au superlattices.

In this paper we report preliminary results from the growth of ultrathin bcc-Co films by MBE on Au(0 0 1)-*hex*. The Au(0 0 1)-*hex* substrates were obtained by a simple epitaxial thin film process on inexpensive and easy to handle MgO single crystals [17]. The samples were structurally characterized in situ by low energy electron diffraction (LEED), scanning tunneling microscopy (STM) and directional Auger electron spectroscopy (DAES) [21–23]. Ex situ analysis of Au coated samples were performed using the magnetooptic Kerr effect.

2. Experimental details and sample preparation

The experiments were performed in a three-chamber UHV system with a base pressure 3×10^{-11} mbar. The system is equipped with a load-lock facility, quadrupole mass spectrometer (SRC), sputter ion gun (Varian), home built MBE evaporators, a reverse view 4-grid LEED/AES optics (OCI), and a room temperature STM head (Burleigh). The samples were deposited on $5\times10\times1$ mm^3 MgO(0 0 1) (Kristallhandel Kelpin) substrates clamped to a Ta plate. The substrates, cleaved ex situ in pure N_2 atmosphere prior to the introduction into the UHV systems, were annealed at 600 °C for 1 h. Metals were evaporated from BeO crucibles heated with a wrap-around tungsten coil. The evaporator assembly was embedded in a water-cooled shroud. The deposition rate was calibrated from the indication of a quartz thickness monitor, which could be placed precisely at the sample position. During the whole deposition process, the pressure in the chamber was maintained in the low 10^{-10} mbar range.

The substrate was a 300 Å (0 0 1)Au buffer layer obtained in a multistage process on a 40 Å Cr seed layer [17]. This way of preparation resulted in a typical Au(0 0 1)-(28×5) reconstruction, so called Au(0 0 1)-*hex*, seen in the STM images as 14.4 Å spaced ridges running along $\langle1\,1\,0\rangle$ Au directions on large atomically flat terraces (compare Fig. 4a).

The cobalt films (a standard thickness of 8 Å and 16 Å was used), were deposited at 300K at the rate of about 1 Å/min. Following the deposition, the Co films were characterized in situ by STM, LEED and the directional Auger electron spectroscopy (DAES) [21,22], referred more generally as the primary-beam diffraction modulated electron emission (PDMEE) [23]. The method involves a strong changes in the Auger yield, when the incidence angle is varied. Scattering interference of the primary exciting electrons gives the strong forward-focusing effect and the maxima of the DEAS polar proliles directly reflect the symmetry and the degree of local order with chemical sensitivity. The DAEA experiment was performed using a standard LEED/AES 4-grid optics (OCI) and the lock-in detection. The magnetic characterization was made applying ex situ magnetooptic Kerr measurements, for which the Co films were covered with a 50 Å Au cap-layer.

3. Results and discussion

Fig. 1 shows LEED patterns for the Au substrate (a) and for the 8 Å Co film (b). Clearly, the square surface mesh of the Co film matches the atomic distance of the Au substrate. In the accuracy limit of our qualitative LEED, the square surface Co mesh has the lattice constant 2.85 ± 0.05 Å which fits in between the expected value 2.82 Å of bcc Co [1] and the value 2.88 ± 0.01 Å found by Wu et al. [20] for Co/Au(0 0 1) superlattices. From the present crystallographic characterization we are not able to exclude a small tetragonal distortion, which in fact means a bct phase. Similar diffraction patterns were also observed for 16 Å films but contrary to the 8 Å films, very weak reflexes with sixfold symmetry

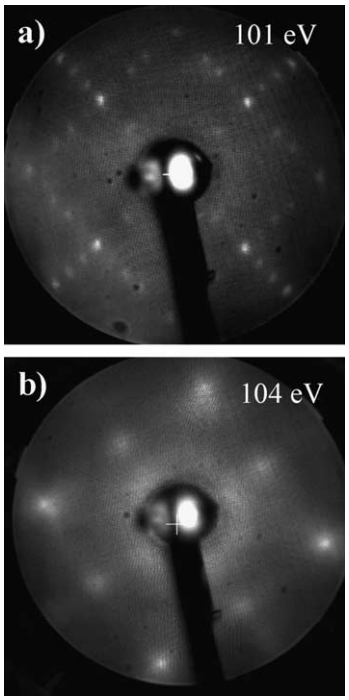

Fig. 1. LEED patterns from the Au(0 0 1)-*hex* substrate (a) and from the surface of the 8 Å Co film (b).

additionally appeared after annealing at 300 °C. In certain aspects, the growth of Co(0 0 1) films on Au(0 0 1)-*hex* seen by LEED is similar to that of Fe films on Au(0 0 1)-*hex*, for which Au floats on top of the Fe film and promotes the layer-by-layer growth [17,19,24]. A similar situation is plausible also for the Co films, for which the Au surfactant action might play also an important role in the stabilization of the bcc phase. Recent energetics calculations of Co adatoms on Au(0 0 1) indicate that there is a preference for the Co atoms to be embedded inside the substrate [25]. From the LEED patterns it could not be excluded that the Co films had a strained fcc structure, giving the same pattern symmetry. However, taking into account that the fcc Co lattice constant is $a_0 = 3.545$ Å, the surface primitive unit mesh has sides $a_S = 3.545\ \text{Å}/\sqrt{2} = 2.506$ Å giving the misfit parameter $f = 13\%$ with the Au(0 0 1) substrate ($a_0 = 4.078$ Å, $a_S = 2.884$ Å), which is a rather large value for the pseudomorphic growth.

To finally verify the film structure we performed the DAES experiment. The intensities of the Au 69 eV Auger line for the Au(0 0 1) substrate and Co 777 eV line for the 8 Å Co film measured as the function of the primary beam (1.4 keV) incidence angle along the [1 0 0] and [1 1 0] azimuths of the Au substrates are shown in Figs. 2 and 3, respectively. The angular distributions for the Au substrate reflect typical features of the fcc lattice, with the intensity maxima corresponding to the dense-packed directions, as shown in the accompanying structural models. The angular distributions measured for the 8 Å Co film clearly show that its structure is bcc (or slightly distorted bcc). They reveal for both azimuths all characteristic features corresponding to the bcc structure of the Co films with the main crystallographic in-plane cubic axis rotated with respect to the fcc Au(0 0 1) substrate by 45°, in agreement with the LEED patterns. Additional weak maxima at 18° and 45° along the

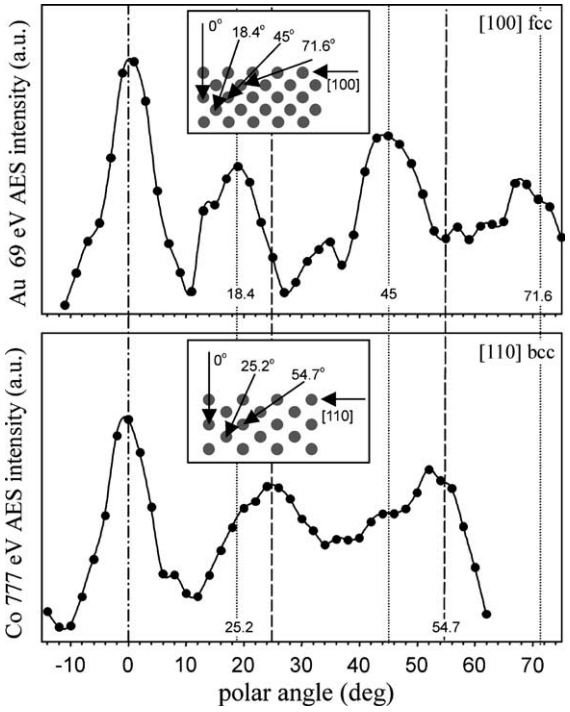

Fig. 2. The normalized intensity of the Au 69 eV and Co 777 eV Auger lines measured for the Au(0 0 1) substrate and the 8 Å Co film, respectively, as the function of the primary beam incidence angle along the [1 0 0] azimuth of the Au substrates. The insets show the models explaining the expected peak positions for the [1 0 0]fcc (top) and [1 1 0]bcc (bottom) azimuths.

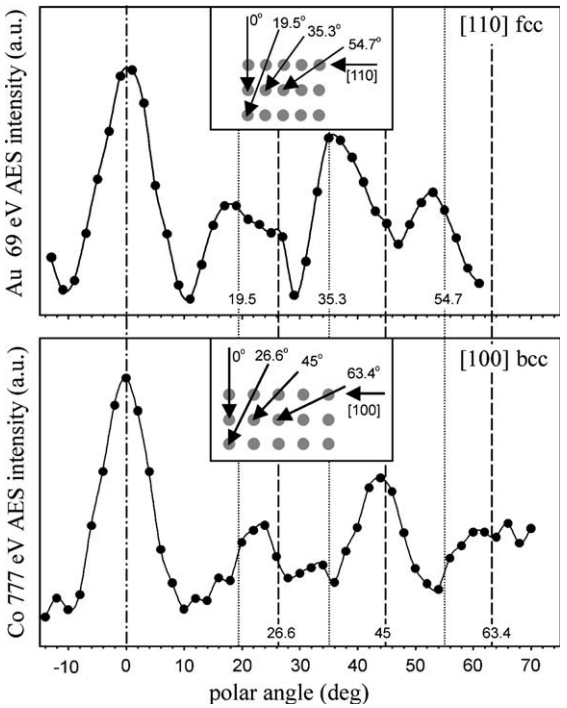

Fig. 3. The normalized Auger intensity of the Au 69 eV and Co 777 eV lines measured for the Au(0 0 1) substrate and the 8 Å Co film, respectively, as the function of the primary beam incidence angle along the [1 1 0] azimuth of the Au substrates. The insets show the models explaining the expected peak positions for the [1 1 0]fcc (top) and [1 0 0]bcc (bottom) azimuths.

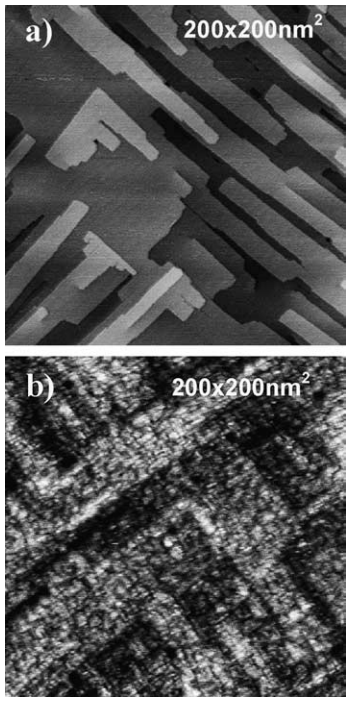

Fig. 4. In situ STM images from the Au(0 0 1)-*hex* substrate (a) and from the surface of the 8 Å Co film (b).

[1 1 0]bcc and at 35° along the [1 0 0]bcc azimuth might be interpretable by a more rigorous modeling of the scattering process. Substrate-like maxima in the overlayer intensity angular distribution can be also induced by back scattering effects or by some degree of substitutional interfacial intermixing. Although the system is thermodynamically immiscible, the equilibrium considerations often fail at the interfaces of ultrathin films, where kinetic effects become important. From the directional AES experiment the bcc structure is also evident for the 16 Å films.

The film surface morphology was checked by in situ STM. The STM images for the Au(0 0 1) substrate and for the 8 Å (about 6 atomic layers) film are shown in Fig. 4. As could be expected from the strong background and broadened spots in the LEED patterns, the surface of the Co films appears grainy but rather flat—maximum only three atomic levels are exposed. The lateral dimensions of the grains are 50–100 Å and the minimum step height is about 1.5 Å. The grains have often elongated rectangular shapes, with the rectangle sides oriented along ⟨1 1 0⟩ directions of Au. The STM images suggest an island growth that is strongly influenced by the reconstruction ridges of the Au substrate.

Magnetic properties of the bcc-Co films on nonmagnetic substrates have not been reported before. Unfortunately, we were not able to characterize the bcc-Co films in situ, and for the ex situ MOKE measurements the films had to be protected with an Au layer. However, we do not expect a change in the film structure induced by the Au overlayer. The LEED pattern proved that it was epitaxial and showed the same reconstruction as the substrate Au layer. Thus, it should play a stabilizing role for the bcc-Co structure, similarly as the Fe overlayer does [13].

Fig. 5 shows the longitudinal MOKE loops for the 8 and 16 Å samples with the magnetic field

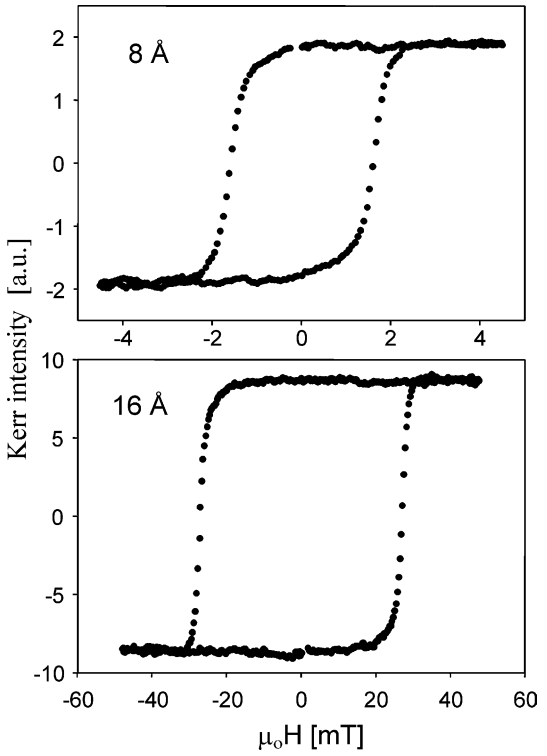

Fig. 5. Longitudal magnetooptic Kerr loops measure ex situ for the 8 and 16 Å bcc-Co films on Au(0 0 1) covered with 5 nm of Au.

applied in the film plane along a ⟨1 0 0⟩ direction of bcc-Co, which showed up to be the easy one for both samples. The samples are fully magnetized in the remanent state and have very low coercive field, which increases by factor 10 for the thicker film. Such a behaviour, rather typical for ultra thin films, is probably connected with the change of the magnetization reversal process from the domain nucleation mechanism to the domain wall movement [26]. The Kerr intensity saturates in a field comparable with the coercive field and especially the thicker film shows a nearly square hysteresis loop. Small in plane anisotropy is probably due to the grainy film structure.

4. Conclusions

The metastable bcc-Co films can be stabilized at room temperature by the molecular beam epitaxy on Au(0 0 1)-*hex* at least up to 10 ML. The films are pseudomorphic with the substrate and the bcc-Co[1 0 0] in plane direction is parallel to the fcc-Au[1 1 0] one. The room temperature growth results in a relatively flat surface (only three atomic levels exposed), displaying granular structures of the monoatomic heights and the lateral dimensions of several nanometers. Down to the smallest investigated thickness (8 Å), the bcc Co films are ferromagnetic at room temperature with the in plane easy axis along the bcc-Co ⟨1 0 0⟩ directions.

Stabilization of bcc-Co on the metallic Au substrate opens unique possibilities of studying relations between the structure and low dimensional magnetism. Due to sharp magnetic interfaces, the system can be used for solving the controversies that arose about the magnetic properties of bcc-Co.

Acknowledgements

This work was partially supported by the Polish State Committee for Scientific Research, grant no. 7 T08A 002 20.

Financial support by The Foundation for Polish Science (FNP) is kindly acknowledged.

References

[1] G.A. Prinz, Phys. Rev. Lett. 54 (1985) 1051.
[2] Y.U. Idzerda, W.T. Elam, B.T. Jonker, G.A. Prinz, Phys. Rev. Lett. 62 (1989) 2480.
[3] P.C. Riedi, T. Dumelow, M. Rubinstei, G.A. Prinz, S.B. Quadri, Phys. Rev. B 36 (1987) 4595.
[4] A.Y. Liu, D.J. Singh, J. Appl. Phys. 73 (1993) 6189.
[5] E. Gu, M. Gester, R.J. Hicken, C. Daboo, M. Tselepi, S.J. Gray, J.A.C. Bland, L.M. Brown, T. Thomson, Phys. Rev. B 52 (1995) 1995.
[6] S.J. Blundell, M. Gester M, J.A.C. Bland, C. Daboo, E. Gu, M.J. Baird, A.J.R. Ives, J. Appl. Phys. 73 (1993) 5948.
[7] J.A.C. Bland, R.D. Bateson, P.C. Riedi, R.G. Graham, H.J. Lauter, J. Penfold, C. Shackleton, J. Appl. Phys. 69 (1991) 4989.
[8] F. Xu, J.J. Joyce, M.W. Ruckman, H.-W. Chen, F. Boscherini, D.M. Hill, S.A. Chambers, J.H. Weaver, Phys. Rev. B 35 (1987) 2375.
[9] Y.Z. Wu, H.F. Ding, C. Jing, D. Wu, G.L. Liu, V. Gordon, G.S. Dong, X.F. Jin, S. Zhu, K. Sun, Phys. Rev. B 57 (1998) 11935.

[10] H. Li, B.P. Tonner, Phys. Rev. 40 (1989) 10241.
[11] S.K. Kim, C. Petersen, F. Jona, P.M. Marcus, Phys. Rev. B 54 (1996) 2184.
[12] G.C. Gazzadi, S. Valeri, Europhys. Lett. 45 (1999) 501.
[13] J. Dekoster, E. Jedryka, C. Mény, G. Langouche, J. Magn. Magn. Mater. 121 (1993) 69;
J. Dekoster, E. Jedryka, C. Mény, G. Langouche, Europhys. Lett. 22 (1993) 433.
[14] P. Blomqvist, R. Wappling, A. Broddefalk, P. Nordblad, S.G.E. te Velthuis, G.P. Felcher, J. Magn. Magn. Mater. 248 (2002) 75.
[15] S.K. Kim, F. Jona, P.M. Marcus, Phys. Rev. B 51 (1995) 5412.
[16] C.P. Wang, S.C. Wu, F. Jona, P.M. Marcus, Phys. Rev. B 49 (1994) 17385.
[17] N. Spiridis, J. Korecki, Appl. Surf. Sci. 141 (1999) 313.
[18] V.L. Moruzzi, P.M. Marcus, K. Schwarz, P. Mohn, Phys. Rev. B 34 (1986) 184;
V.L. Moruzzi, P.M. Marcus, K. Schwarz, P. Mohn, J. Magn. Magn. Mater. 54–57 (1986) 955.
[19] O.S. Hernan, A.L.V. de Parga, J.M. Gallego, R. Miranda, Surf. Sci. 415 (1998) 106.
[20] L. Wu, K. Shintaku, T. Shinjo, N. Nakayama, J. Phys.: Condens. Matter 5 (1993) 6515.
[21] S. Mróz, M. Nowicki, Surf. Sci. 297 (1993) 66.
[22] S. Mróz, Surf. Rev. Lett. 4 (1997) 117.
[23] S. Valeri, A. di Bona, G.C. Gazzadi, Surf. Interface Anal. 21 (1994) 852.
[24] V. Blum et al., Phys. Rev. B 59 (1999) 15966.
[25] V.S. Stepanyuk, W. Hergert, P. Rennert, Comp. Mater. Sci. 17 (2000) 309.
[26] M. Kisielewski, Z. Kurant, A. Maziewski, M. Tekielak, N. Spiridis, J. Korecki, Phys. Stat. Sol. (a) 189 (2002) 929.